

Reservoir computing using arrayed waveguide grating

Chun Gao

Centre for Optical and Electromagnetic
Research, State Key Laboratory for
Modern Optical Instrumentation
Zhejiang University
Hangzhou, China
22130068@zju.edu.cn

Xiaowan Shen

Centre for Optical and Electromagnetic
Research, State Key Laboratory for
Modern Optical Instrumentation
Zhejiang University
Hangzhou, China
12130066@zju.edu.cn

Xinxiang Niu

Huawei Technologies Co., Ltd
Shenzhen, China
niuxinxiang@huawei.com

Yajie Li

Huawei Technologies Co., Ltd
Shenzhen, China
liyajie5@huawei.com

Zejie Yu

Centre for Optical and Electromagnetic
Research, State Key Laboratory for
Modern Optical Instrumentation
Zhejiang University
Hangzhou, China
zjyu@zju.edu.cn

Yiwei Xie

Centre for Optical and Electromagnetic
Research, State Key Laboratory for
Modern Optical Instrumentation
Zhejiang University
Hangzhou, China
xieyiw@zju.edu.cn

Xiaowen Dong

Huawei Technologies Co., Ltd
Shenzhen, China
xiaowen.dong@huawei.com

Huan Li

Centre for Optical and Electromagnetic
Research, State Key Laboratory for
Modern Optical Instrumentation
Zhejiang University
Hangzhou, China
lihuan20@zju.edu.cn

Daoxin Dai

Centre for Optical and Electromagnetic
Research, State Key Laboratory for
Modern Optical Instrumentation
Zhejiang University
Hangzhou, China
dxdai@zju.edu.cn

Abstract—We proposed a 32-channel 50G AWG as the core device to implement the on-chip optical reservoir computing. With appropriate iterative mode and output-level training strategy, the chip has achieved good results in predicting Macky-Glass series. For sequences of 1000 length, this type of optical reservoir calculation can obtain an absolute error of about 0.02 and a relative error of 0.018.

Keywords—Optical computing, Reservoir computing, Arrayed waveguide grating

I. INTRODUCTION

Reservoir computing (RC) is a kind of recurrent neural network (RNN) with a special structure^[1]. As can be seen from Fig. 1, Unlike traditional RNNs where every parameter in the network is trainable, most of the parameters of the reservoir computing have fixed weights. Only the output stage in the network can be changed during the training process, which gives reservoir computing a unique advantage for photonic network implementation. First, the fixed network structure eliminates the need for photonic chips with fully reconfigurable topologies such as Clements^[2] and Reck^[3], greatly reducing the area of the chip and the required circuit inputs. Secondly, compared with the previous photonic neural networks, which require backpropagation through external calculations, the training mode of reservoir computing without backpropagation is more suitable for photonics realization. Third, reservoir computing has a high tolerance for the form and error of matrix, which means that it has high flexibility for integrated photonics design and fabrication, and can realize the calculation function based on widely used photonics devices, such as delay lines^[4].

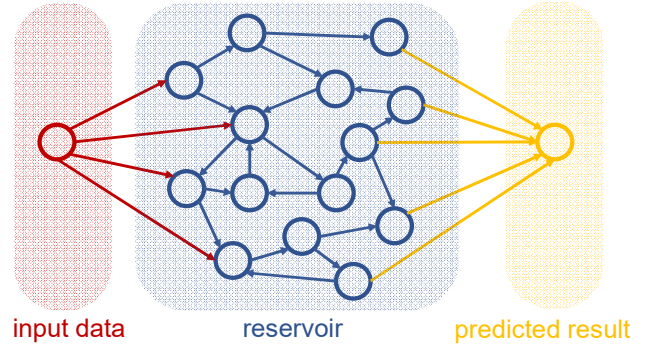


Fig. 1. Schematic diagram of the reservoir computing

$$x_{res}(t+1) = W_{in} \cdot x_{in}(t+1) + W_{res} \cdot x_{res}(t) \quad (1)$$

An arrayed waveguide grating (AWG) is a common wavelength division multiplexing (WDM) device^[5], which, in this work, is used as the physical implementation of the matrix calculation of the reservoir iteration. As indicated by Eq. (1), the iteration of each step of the reservoir computing consists of two parts, one is to realize the alignment of the dimensions of the input signal and the reservoir through the input matrix. The other is the product of the refreshing matrix and the reservoir at the previous moment, and the result of the addition of these two parts is the state of the reservoir at this moment. Compared with traditional MZI networks and on-chip diffraction neural networks, this AWG-based RC structure can greatly reduce the area of the chip and the overall insertion loss.

II. DESIGN, FABRICATION AND PACKAGING

A tailored design of 32-channel 50G AWG is adopted to implement reservoir computing. After the light enters the chip

through the grating couplers, it will first enter the 32-channel power splitter as a coherent input. Subsequent thermo-optic MZI array and phase-modulation array load the reservoir state into the AWG in a complex form. Common ground is chosen in the circuit design of the chip, and at the same time, the largest possible ground electrode ensures the smallest possible voltage crosstalk. In the arrayed waveguides of the AWG, there are also microheaters used to change the weight of the reservoir matrix. Figure 2 is the overall layout of the chip. The final packaged chip is shown in Fig. 3.

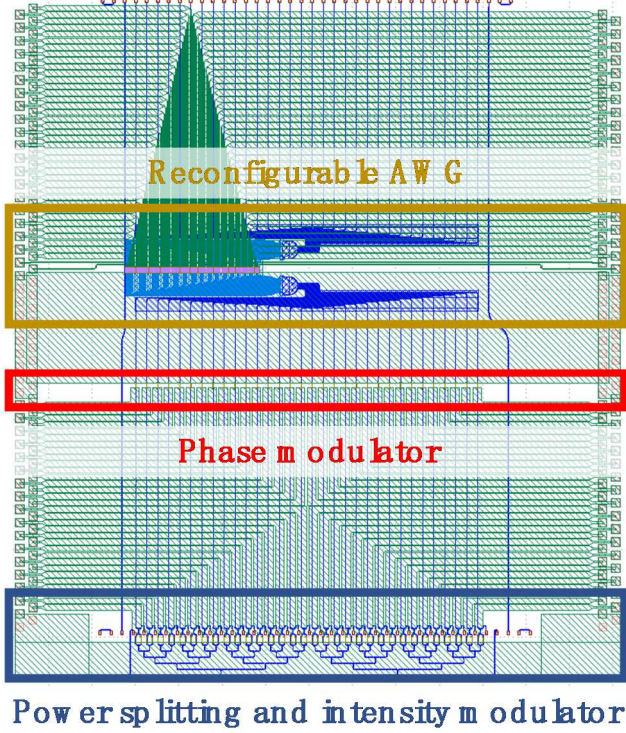


Fig. 2. Layout design of the chip

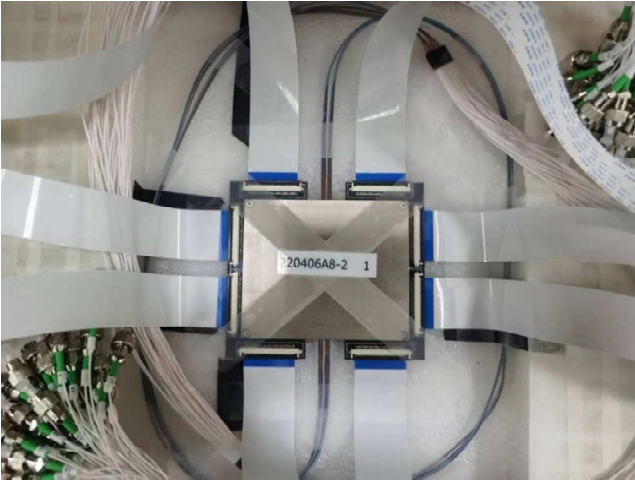


Fig. 3. A photo of the packaged chip

III. IMPLEMENTATION METHOD OF RESERVOIR COMPUTING

The process of using this chip to realize the reservoir computing is demonstrated in Fig. 4.

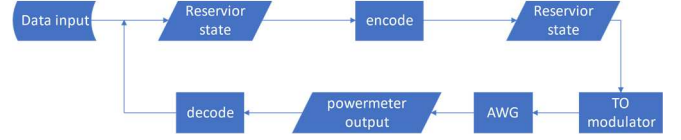


Fig. 4. Flowchart for realizing optical reservoir computing

In each iteration, the output of the optical chip needs to be obtained by a power meter, and then decoded and superposed on the input signal, and then encoded and loaded onto the microheaters of the modulator. This "encoding-decoding" process has a high degree of freedom, which affords this reservoir system rich dynamic characteristics and can be optimized according to different temporal characteristics.

During the training process, after obtaining all the states of the reservoir for a certain time interval, the weighted data of the output level can be obtained by the ridge regression algorithm. The weights of the output stage can also be updated by a backpropagation algorithm similar to RNNs. The peripheral circuit of the chip will act as an output stage, converting the output of the chip into a predicted result.

IV. RESULTS AND FUTURE PROSPECTS

The experiment utilized Macky-Glass (M-G) series as data for training and testing. Because the process of reservoir iteration and prediction can be independent, several sets of experiment data are collected first, then the analysis is done by manually dividing the training set and the test set after the experiment. In this experiment, the output optical power is first decoded to a scale similar to the reservoir data by a linear transformation, and then added to the input signal and encoded to the corresponding voltage input by a similar linear transformation to load onto the modulator array. The M-G sequence are one-dimensional data, so the input is a matrix of size (1,32). Each sequence has a length of 1000 steps, of which the first 100 steps serve as the reservoir's initialization. The subsequent data is used for the regression of the output stage.

The prediction results of the MG series are demonstrated in Fig. 5, where the blue line represents the actual data, and the yellow line represents the predicted result. The deviation of the predicted result from the actual data is expressed by the root mean square error (RMSE), which is calculated from Eq. (2). To calculate the relative error, the normalized root mean square error (NRMSE) is used in the experiment. The RMSE and the predicted sequence itself are divided to eliminate the influence of the units of the sequence on the results, just as Eq. (3) indicates. In Fig. 6, the blue line represents the RMSE, and the yellow line represents the NRMSE.

$$RMSE = \sqrt{\frac{\sum_n (y_i - \hat{y}_i)^2}{n}} \quad (2)$$

$$NRMSE = \sqrt{\frac{\sum_n (y_i - \hat{y}_i)^2}{\sum_n y_i^2}} \quad (3)$$

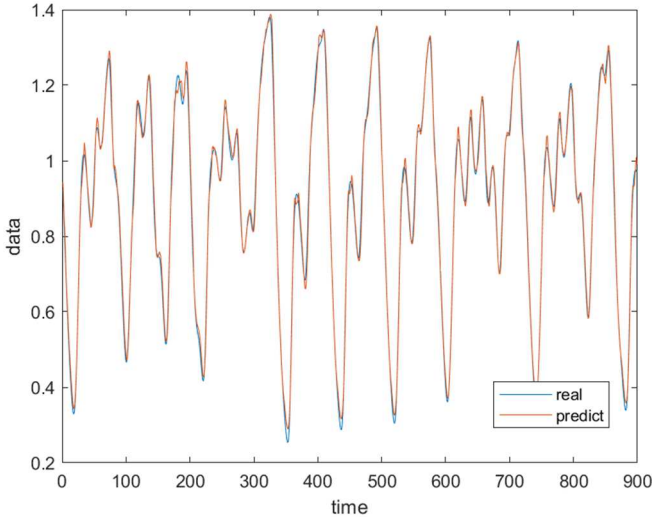


Fig. 5. Real sequence data and results predicted by RC

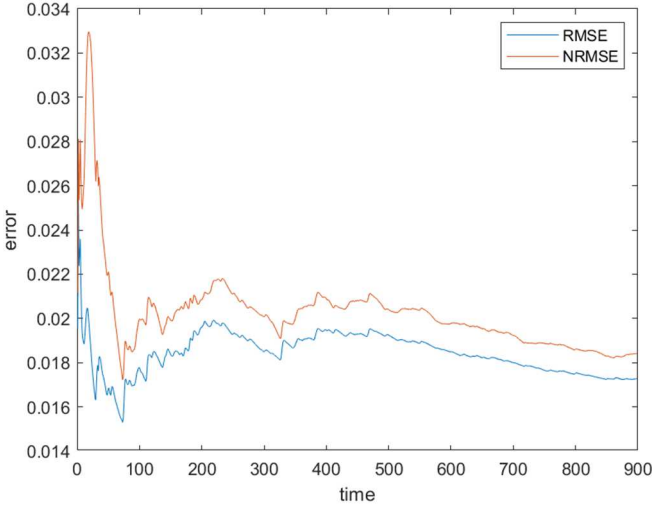


Fig. 6. RMSE and NRMSE for predicted outcomes and real data

As can be seen from Fig. 6, after stabilization, the AWG-based reservoir computing yields an NRMSE of about 0.018.

This shows that this chip architecture can predict near-chaotic temporal sequences such as M-G series.

In future work, we will try to use multi-dimensional, multi-wavelength inputs to maximize the WDM characteristics of AWG to increase the number of nodes in the reservoir. New decoding-encoding methods and output stage structures will also be used to predict the dynamic behavior of the system. In addition, more datasets or even language models will be used in the study.

ACKNOWLEDGMENT

This work is funded by National Key Research and Development Program of China (2021YFB2801700, 2021YFB2801702), National Natural Science Foundation of China (62175214), Leading Innovative and Entrepreneur Team Introduction Program of Zhejiang (2021R01001), Zhejiang Provincial Natural Science Foundation of China (LDT23F04012F05, LDT23F04014F01), and Startup Foundation for Hundred-Talent Program of Zhejiang University.

REFERENCES

- [1] W. Maass, T. Natschlger and H. Markram, "Real-Time Computing Without Stable States: A New Framework for Neural Computation Based on Perturbations," in *Neural Computation*, vol. 14, no. 11, pp. 2531-2560, 1 Nov. 2002.
- [2] W. R. Clements, P. C. Humphreys, B. J. Metcalf, W. S. Kolthammer and I. A. Walmsley, "Optimal design for universal multipoint interferometers," in *Optica*, vol. 3, no. 12, pp. 2334-2536, 23 May. 2016.
- [3] M. Reck, A. Zeilinger, H. J. Bernstein and P. Bertani, "Experimental realization of any discrete unitary operator," in *Phys. Rev. Lett.*, vol. 73, no. 1, pp. 58, 11 Feb. 1994.
- [4] K. Vandoorne, P. Mechet, T. V. Vaerenbergh, M. Fiers, G. Morthier, D. Verstraeten and et al, "Experimental demonstration of reservoir computing on a silicon photonics chip," in *Nat Commun*, vol. 5, no. 1, pp. 1-6, 24 Mar. 2014.
- [5] S. Pathak, D. V. Thourhout and W. Bogaerts, "Design trade-offs for silicon-on-insulator-based AWGs for (de)multiplexer applications," in *Optics Letters*, vol. 38, no. 16, pp. 2961- 2964, 15 Aug. 2013.